PORT SAID ENGINEERING RESEARCH JOURNAL

Faculty of Engineering - Port Said University
Volume 27 No. 4 pp: 25:33

Dynamic Analysis of Wheel-Rail Interaction Stress Distribution for ENR Locomotives

Ahmed Adel Turk[1], *Ismail Mohsen* [*2,] *and Ashraf El-Sabbagh*[3]

[1] *Civil Engineering Department, Faculty of Engineering, Port Said University, Port Said, Egypt*, email: *ahmed.adel@eng.psu.edu.eg*

[2] *Civil Engineering Department, Faculty of Engineering, Port Said University, Port Said, Egypt*, email: *ismail99614@eng.psu.edu.eg*

[3] *Civil Engineering Department, Faculty of Engineering, Port Said University, Port Said, Egypt*, email: *ashref.ismail@eng.psu.edu.eg*

**Corresponding author, DOI: 10.21608/PSERJ.2023.234600.1259*

Received 7-9- 2023
Revised 21-9- 2023
Accepted 1-10- 2023

ABSTRACT

Egyptian rails have gotten worn as a result of a lack of upkeep and inadequate rail grinding. If the new locomotives are designed to work with standard tracks, they should be able to move more efficiently and safely on standard rails than worn ones that were not designed for standard tracks. The contact stress variation brought on by variations in the wheel-rail contact profile has a significant impact on the safety of railway traffic. In this article, a standard rail UIC54 and a wheel profile as per Egyptian Railway standards are taken into consideration to explore the impact of interacting wheel and rail profile topology. Standard rail and a real worn rail from the Egyptian National Railways (ENR) have different rail profile radii. The problem is undertaken using ANSYS Finite Element Method (FEM). All required elements of the rail system were modeled for analyses., such as rail, wheel, and axle. These tools obtain the distribution of contact stress, contact pressure, and fatigue for standard and damaged rail profiles. Using stress distribution obtained through FEM analysis, the effects of the change in Egyptian rail profiles with ENR New locomotives' wheel on the contact stress is investigated. Contact stresses for the worn rail profile are up to 40% lower than those for an unused ENR rail profile. As the worn rail has a larger contact area than the standard rail, there is a reduction in the life cycles to failure., and fatigue damage rises as the contact stresses decrease.

Keywords: Wheel-rail contact stresses, Finite Element Analysis, wear, ANSYS

1 INTRODUCTION

Rail defects are a common problem in Egypt's railway system, which can pose serious risks to passenger safety and cause disruptions to the country's transportation network. Any imperfection or damage to the rail infrastructure that might compromise its overall strength, durability, or performance is referred to as a track problem.

Examples of common types of rail defects in Egypt include worn rails, defective joints or welds, and broken or missing fasteners such as clips, bolts, and screws. These defects can occur due to various reasons such as heavy or insufficient investment in the railway system.

Egyptian rails have gotten worn due to a lack of upkeep and inadequate rail grinding. If the new locomotives are designed to work with standard tracks, they should be able to move more efficiently and safely on standard rails than worn ones not designed for standard tracks.

All studies on how vehicles and tracks interact are built around a wheel's contact with a rail. Through the process of the stresses it transmits, this small interface controls the dynamic performance of locomotives. It is vulnerable to severe damaging occurrences, much like any area of high stress. To accurately simulate vehicle dynamics and conduct damage studies, it is crucial to understand the mechanism of contact through wheel and rail. The Hertz technique has been used extensively in research on contact interaction in a pair of wheel rails[1]. The Hertz hypothesis has served as the foundation for several analytical techniques that have been developed to study the contact between moving wheel-rail surfaces. Several scholars have developed a way to determine the equation of Hertz for contact area, penetration, and contact pressure. [2]. By getting close to the elliptic axis ratio, the researchers have tried to numerically simplify the solution to the elliptic integral. Tanaka developed a new technique for calculating elliptical Hertz contact pressure that does not need the calculation of an elliptic integral[3]. polynomial estimation was used in place of the elliptical integral to generate a hypothetical Hertzian contact model[4]. The elliptical integral was simplified by the researchers using an innovative method, and the outcome exhibits good agreement with the theoretical findings. In addition to employing analytical-numerical approximation, FEM was used in the year 2000 to solve the Hertzian contact issue related to wheel-rail contact[5]. Three different approaches, namely the Hertz theory, FEM, and software contact from Kalker, have been used to compare the contact pressure calculations. Next, FEM and the quasi-Hertz approach have been used to model the results of the interaction between wheel and rail surfaces on how contact stresses and zones are distributed [6]. Scientists have attempted to resolve the Hertzian contact for the minute radius of curvature using analytical as well as FE modeling to evaluate the adjustment of the highest stress of contact in the rail concerning the change in rail radii of curvature [7]. Wheel and rail contacting profiles deteriorate over time due to wear. Abrasion, also and surface plastic distortion are both included. The change in the geometry profile affects the stress distribution over the rail. To calculate the change in the rail profile a 3D digital model is used. Thanks to various recent technical advancements, 3D digital models of components have become more useful for tracking the progression of wear in mechanical and biological applications[8][9], [10]. As the government has brought new locomotives to work with the damaged rails, we need to find out the effect of the worn rails on the contact stresses with standard locomotive wheels. If the new locomotives are designed to work with standard tracks, they should be able to move more efficiently and safely on standard rails than worn ones. The study takes a thorough approach to the subject, starting with a theoretically grounded analytical examination of the contact involving the wheel and the rail using Hertz's hypothesis of contact. Standard UIC54, real worn UIC54 rail profiles, and a standard wheel are used to evaluate the effect of the ENR worn rails on stress analysis with new locomotives.

2 METHODOLOGY

Using finite element software (ANSYS), the study was divided into two main parts. The following methodology was used to meet the aim of the research:

- By first checking earlier mathematical models, and FE procedures, and validating results by simulating the interaction between wheel and rail using finite element software (ANSYS).
- After that, create a simulation model using ANSYS to show the effects of worn rails on the change of stress distribution due to the interaction between wheel and rails for ENR locomotives with the help of a case study at Port-Said railway tracks.

2.1 Wheel-rail Contact Model Using Mathematics

Heinrich Hertz, a German scientist who developed the Hertzian Contact Hypothesis in the year 1882, gave it that name. It includes hypotheses that lay the theoretical groundwork for the wheel-rail steady-state contact under rolling situations. Calculations of contact stresses and contact geometry are done using the theory of elastic deformation. The contact region between two elastic nonconforming objects adopts an elliptical shape with a half-major axis (a) along with a half-minor axis (b) as determined by the researchers. [11]. The distribution of the amount of pressure from contact in this elliptical area in Figure (1) represents a semi-ellipsoid, expressed as:

$$p = p_o\sqrt{\left(1-\frac{x^2}{a^2}-\frac{y^2}{b^2}\right)} \quad (1)$$

$$a = m\left[\frac{3\pi}{4}\frac{P(K_1+K_2)}{A+B}\right]^{1\backslash 3} \quad (2)$$

$$b = n\left[\frac{3\pi}{4}\frac{P(K_1+K_2)}{A+B}\right]^{1\backslash 3} \quad (3)$$

Where K_1 and K_2 are constants that depend on the material properties of railway wheel and rail respectively.

$$k_1 = \frac{1-\upsilon_1^2}{\pi E_1} \quad (4)$$

$$k_2 = \frac{1-\upsilon_2^2}{\pi E_2} \quad (5)$$

Where υ_1 and E_1 are Poisson's ratio and young's modulus of the railway wheel material and υ_2, and E_2 are Poisson's ratio and young's modulus of railway rail material.

Understanding some of the mathematical constants used in the formula above is necessary for calculating the contact areas.

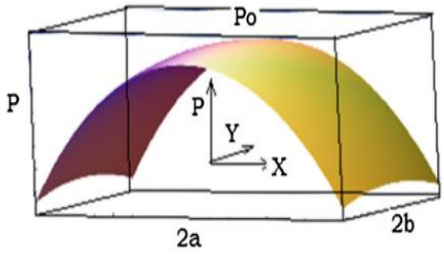

Figure 1: Pressure distribution across the elliptic area

The next curved ratios are connected in terms of a wheel-rail combination:

$$A+B = \frac{1}{2}\left(\frac{1}{R_{11}}+\frac{1}{R_{12}}+\frac{1}{R_{22}}+\frac{1}{R_{21}}\right) \quad (6)$$

$$B-A = \frac{1}{2}\left[\left(\frac{1}{R_{11}}-\frac{1}{R_{12}}\right)^2+\left(\frac{1}{R_{22}}-\frac{1}{R_{21}}\right)^2+\ 2\left(\frac{1}{R_{11}}-\frac{1}{R_{12}}\right)\left(\frac{1}{R_{22}}-\frac{1}{R_{21}}\right)\cos 2\psi\right]^{1\backslash 2} \quad (7)$$

where A and B are positive constants. The four most important relative curvature radii are R11, R12, R21, and R22.

Figure (2) provides a visual representation of this idea. R21 is the runway's radius, which in this case is infinite, and R22 is the rail's curvature in the cross-sectional plane. R11 is the curvature of the rolling radius of a wheel. R12 is the wheel profile radius, which for a conical wheel goes to infinity. The factors "m" and "n" relate the mathematical parameter A/B with the ellipticity parameter a/b. The notation reads cos=(B-A)/(A+B) The amounts of m and n for different values are calculated using the tables.[12]. Regression is used to obtain the intermediate values utilizing the most effective curve-fitting method, as illustrated in Figures (3), and (4).

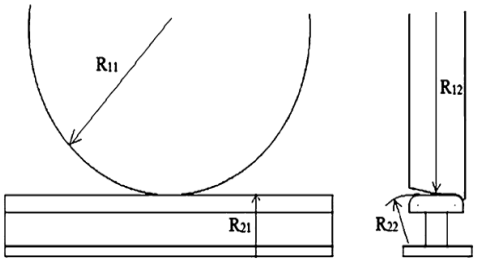

Figure 2: Wheel rail arrangement illustrating several major curvatures.

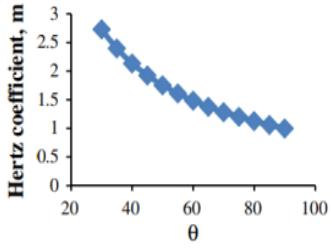

Figure 3: Hertz coefficient, "m," and " θ " on a graph.

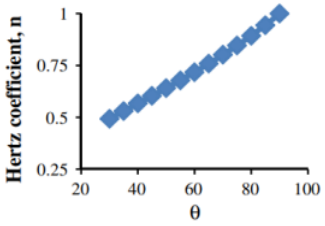

Figure 4: Hertz coefficient, "n," and " θ " on a graph.

2.2 Contacting profiles

In Egypt, the UIC54 rail is the most often used. Its transverse head profile is shown in Figure (5) as a collection of circular curves with varying radii of 13, 80, and 300 mm. The components of the profile on the 13,80, and300 mm radii are, respectively, the rail gauge corner, rail shoulder, and rail crown. The transverse movement of the wheel may cause first contact to occur on each section of the profile. In this paper contact nearby of radius 300 is taken into account with the wheel tread. The profile radii can change over time as a result of surface wear and plastic deformation. To investigate the influence of the rail profile's change on contact stresses, pressure, and fatigue lifetime for both static and dynamic conditions a standard ENR UIC54, a real worn ENR UIC54 rail profile from ENR, and a wheel profile as per Egyptian standards are used as shown in figure (6).

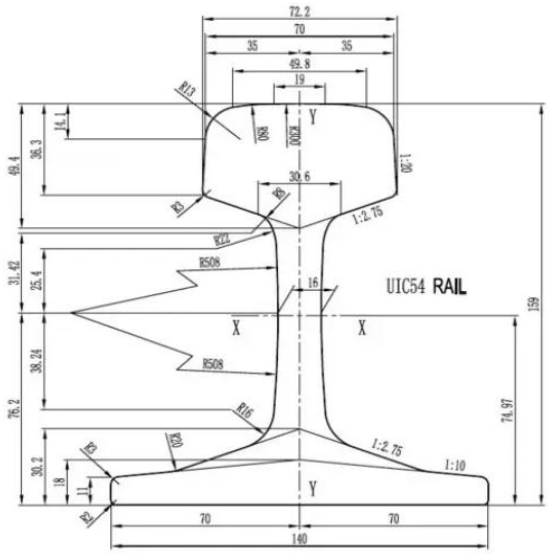

Figure 5: UIC 54 rail profile

Figure 6: Profile of wheel as per ENR standards

2.3 FEA Procedure

An AutoCAD environment within Solid Works was used for geometric modeling. After that, the geometry was loaded into the FE ANSYS as illustrated in figures (7), and (8). Due to its linear structure, the contact issue takes a long time to process.

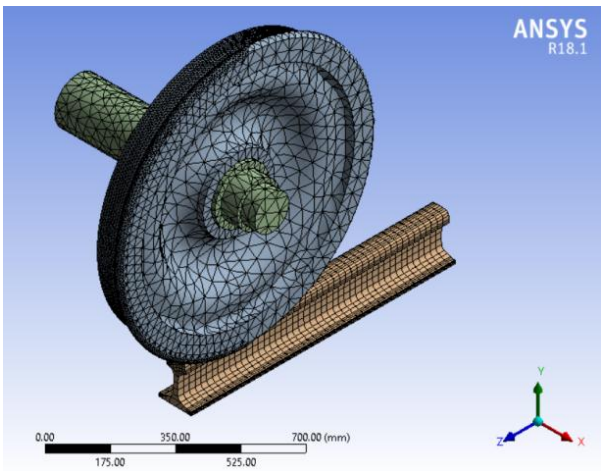

Figure 7: The wheel-rail assembly's FE model

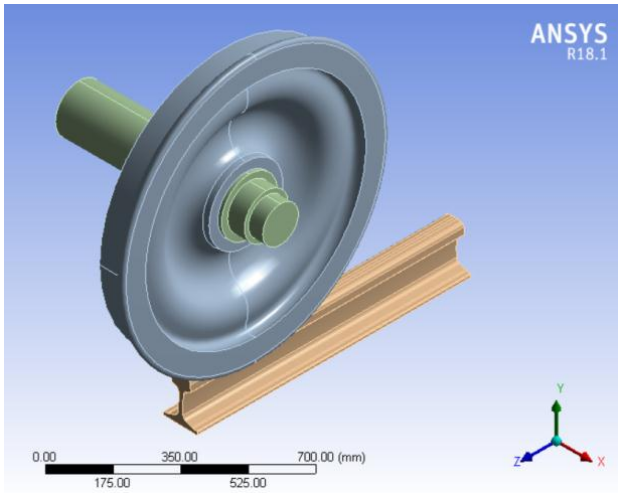

Figure 8: Wheel-rail assembly geometric model

Two points of contact were established: (1) between the rail and the wheel; and (2) between the wheel and the axle. Frictional contact was attributed to the rail and wheel interface, with a coefficient of friction of 0.3. Additionally, the interface of contact between the axle and the wheel was described as frictionless. Because the rail is generally flat and the curvature of the wheel at the contact is convex, it is chosen to be the target body and the contact body. The initial interaction between the wheel and the hub exhibits frictionless behavior, allowing for sliding without energy waste. The model's inclusion of an axle brings the work closer to reality. Here, the outside surface of the axle is made contact while the perimeter of the wheel is targeted. As a result, the contact body is the smaller surface and the larger surface is the target body. The rail's cant angle is captured at 1:40. During the study, The wheel was rotated around its axis to imitate movement on the rail. The wheel revolved around the axle since they were bound together, and motion was created through the friction between the wheel and rail. To fix the assembly, fixed supports were attached to the rails' bottom surface. By choosing the surfaces that interact with the rails and wheels, the model has been divided into the face-sizing mesh which governs only the contact faces of the rail and wheel. Using a finer mesh increases accuracy but also requires more computational resources. Results are almost the same when using 7,6,5 mm mesh so refining the mesh further may not lead to substantial improvements in accuracy. As a consequence, it was given Tet mesh and the size for meshing has been set up to 5mm so that the accurate result may be achieved as in previous work [13][14]. Fine relevance adjustments were applied to the remaining bodies so that they would have a decent mesh with a growth rate of 1.2. The body-colored mesh was created with a 0.0004476 m minimum edge length. The FE model has a total of 177247 nodes and 110470 elements. the total carload is 80 tons. Since there are 8 wheels, the weight that each one applies to the rail is 10 tonnes (or around 100 KN). Gravity was taken into account in the study, but the load was distributed evenly

across the points at the wheel's carrying location where the axle is placed. Horizontal external forces were ignored aside from actual contact conditions because of the cant angle. using the identical material data, elasticity modulus, E= 207GPa and 205GPa for rail and wheel respectively, and Poisson's ratio, υ = 0.3. It is assumed that the rail and wheel are linearly elastic.

2.4 Analysis of Fatigue

Based on the results of the FE study, this part gives the estimate for fatigue life. Three phases are often used to describe the life of a fatigue crack: crack start and development. These three phases include Phase 1, which is surface shearing stress-driven beginning, Phase 2, which is transitory cracking behavior, and Phase 3, which is the phase after tension and fracture-driven propagation of cracks. Fracture first manifests at moving contact points as a result of accumulated deformation caused by shear from multiple rolling-sliding contact stresses [15]. When phase 1 is finished, initiation may be seen to have happened. Jiang suggested using a straightforward damage factor for a fatigue lifetime calculation [16].

Table (1) The mechanical characteristics of the rail and wheel material

E Rail (GPa)	E Wheel (GPa)	υ
207	205	0.3

2.5 Case Study and Measuring Instrument

A 3D laser scanner is used to evaluate wear for the rail profile at the port-said railway station as shown in figure (9). The Leica Scan Station P40 laser scanner offers the highest versatility including long range, speed (up to 1 million points per second), and accuracy (3D positional accuracy of 3mm at 50m and 6mm at 100m). The instrument enables 3D scanned data to be used directly in any CAD software. The worn rail portion in Figure (10) was scanned and carried out in CAD3D-environment figures (11), (12). A cross-section is taken in the rail data points and carried out in Solid work to be extruded for the study as shown in Figure (13).

Figure 9: P40 3D Laser Scanner

Figure 10: worn rail

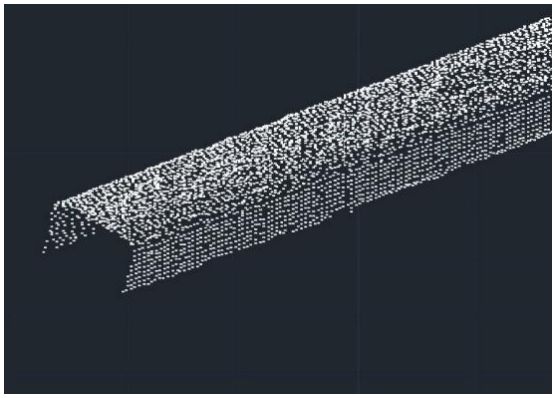

Figure 11: Isometric of the worn railhead

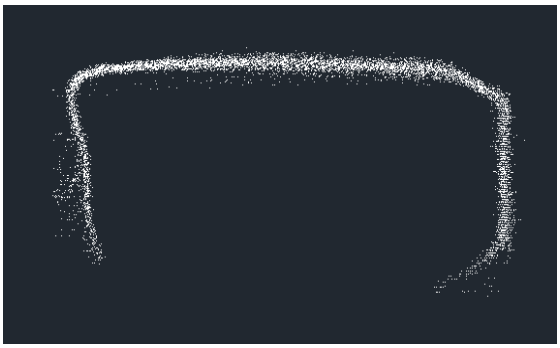

Figure 12: Cross-sectional of the worn railhead

Figure 13: Solid work for a cross-sectional of the worn railhead

After that, the model geometry was loaded into FE ANSYS. The scanning phase targets only the rail head. This research will analyze the assembly when the wheel is positioned on the rail just over the sleeper and the dynamic motion analysis of the wheel on the rail with a velocity of 80 km/h.

3 RESULTS AND DISCUSSION

For the validation of standard UIC54, On the rail surface's top, the contact pattern is shown. Hertzian analytical calculation result for the contact pressure distribution is 1236.6 MPa and as shown in figure (14) the FE result from the software ANSYS is 1210.5 MPa. The FEM result is close to the analytical answer. These results are more realistic and accurate when compared to the calculations obtained in previous studies[17][13].

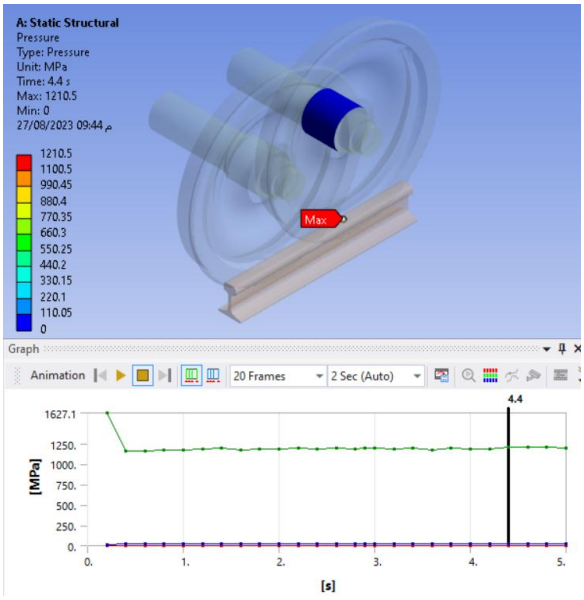

Figure 14: Contact pressure distribution in the contact region

Analysis of both static and dynamic loadings was done. The rail's and wheel's corresponding Von-Mises stress distributions were found. The loading evaluations were done for the wheel when it was just above the sleeper on the rail. The worn rail as well as the standard rail have been examined. As can be seen in Figure (15) the stress on the standard rail is 856.35 MPa. Stress is higher than yield stress. The portions above the yield point suffered permanent deformation, and the head of the rail experienced the start of corrugation development caused by static stress. the contact area's stress distribution is not uniform. Red areas of the contact area cause the most stress while lesser stress is shown elsewhere. This is a consequence of the different contact profiles of the rail and wheel. Compared to the stresses from earlier research, these results are more accurate and realistic[13][18]. the Von-Misses stress of the worn rail is 523.46 MPa as shown in figure (16). The worn profile was discovered to have lower contact stresses than the standard which matches previous work[19]. Contact stresses for the worn rail profile are up to 40% lower than those for an unused ENR rail profile. Compared to the standard rail, the worn rail has a larger radius of curvature. This explains the findings since lower stresses are created with larger contact areas when the same load is applied. In general, terms, when a load causes two surfaces with differing

curvature radii to come into touch, the surface with the smaller radius of curvature tends to experience higher contact stress in the immediate region of contact. This is because a smaller radius of curvature leads to a smaller contact area, which results in higher pressure (force per unit area), leading to higher stress. As shown in Figures (17), and (18), the contact area for the worn rail is much greater than the contact area of the standard rail.

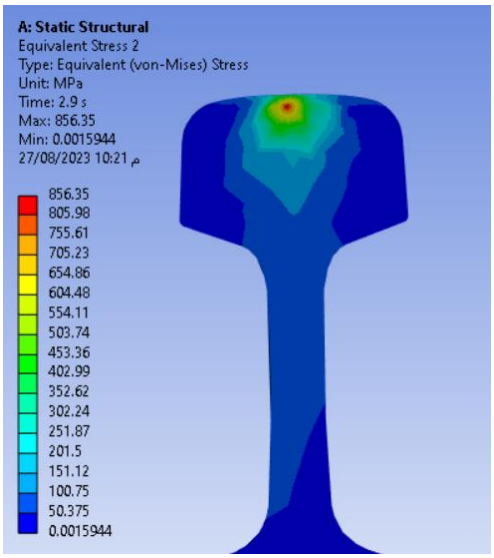

Figure 15: Von-mises stress distribution for standard rail

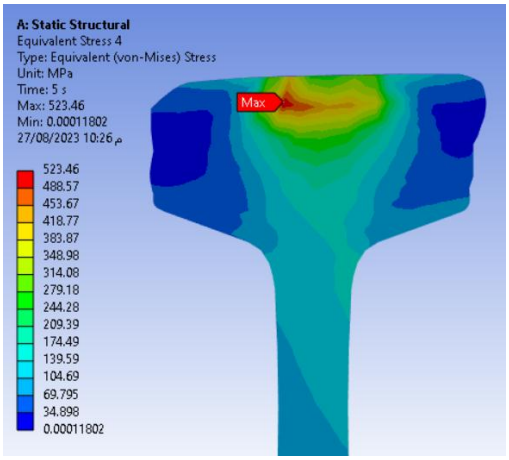

Figure 16: Von-mises stress distribution for worn rail

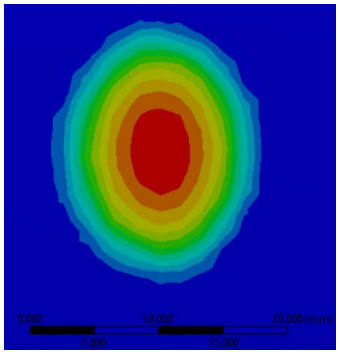

Figure 17: Contact area for standard rail

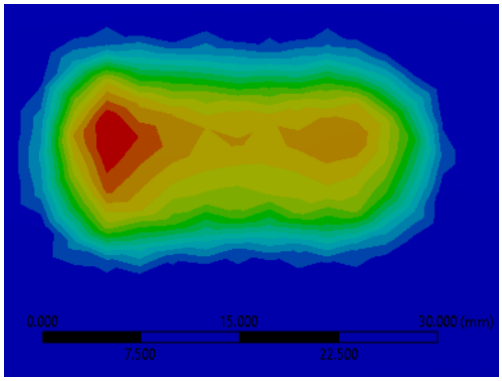

Figure 18: Contact area for worn rail

The most critical location for the beginning of a fatigue fracture is thought to be the highest von Mises stress point. Using FE, for standard and deteriorated rail profiles, damage caused by fatigue and the total number of failure cycles are calculated. The results are regardless of the cracks propagated on the worn rail or any other defects. The FE deals with the rail changes from a profile point of view. Figures (19), (20), (21), and (22) demonstrate that a number reduction in life cycles is found and that the fatigue damage rises as the contact stresses decrease as predicted. Smaller radii of curvature can lead to stress concentration points, where the stress is significantly amplified compared to the average stress in the structure. These stress concentration points are more likely to initiate cracks and other forms of damage, which can eventually lead to fatigue failure. Larger radii of curvature help distribute stress more evenly and reduce the likelihood of stress concentration.

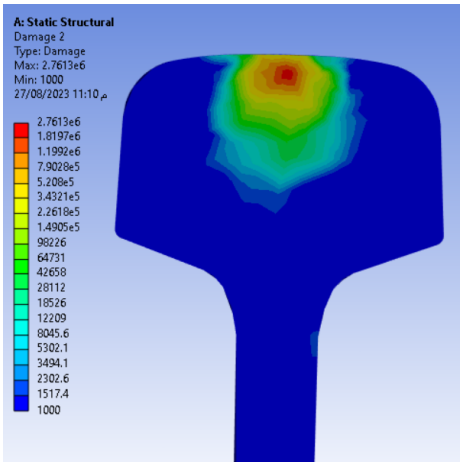

Figure 19: Fatigue damage for standard rail

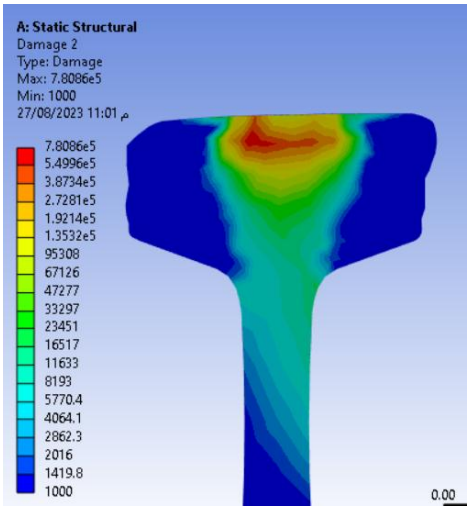

Figure 20: Fatigue damage from worn rail

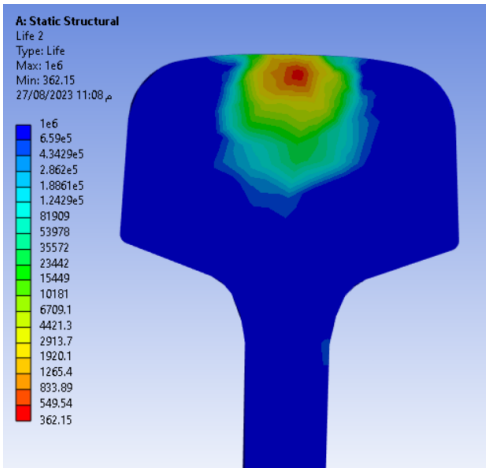

Figure 21: Fatigue life for standard rail

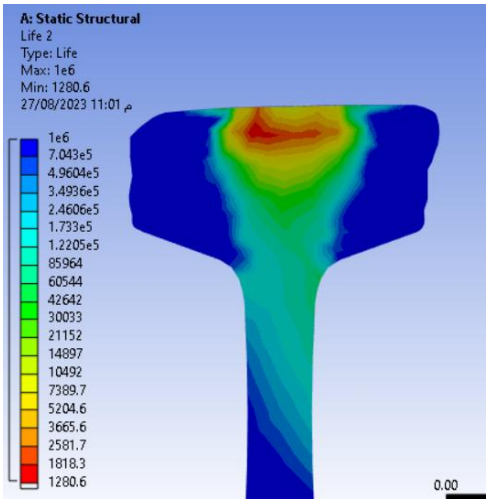

Figure 22: Fatigue life for worn rail

On account of the dynamic relation between the rail and the wheel, analysis was done with the assumption that the wheel velocity was 80 km/h. As shown in figure (23) Von-Misses stress value exceeds the yield stress for both standard and worn rail respectively 2111 MPa and 1114 MPa. The standard profile's contact stresses were found to be higher than those of the worn profile because of the variation of the profile curvature as explained before. The dynamic stress variation for the standard rail is larger than the worn one. the lower stress range means the initiation and propagation of cracks occur at a slower pace. This can result in a longer lifespan for the material before failure.

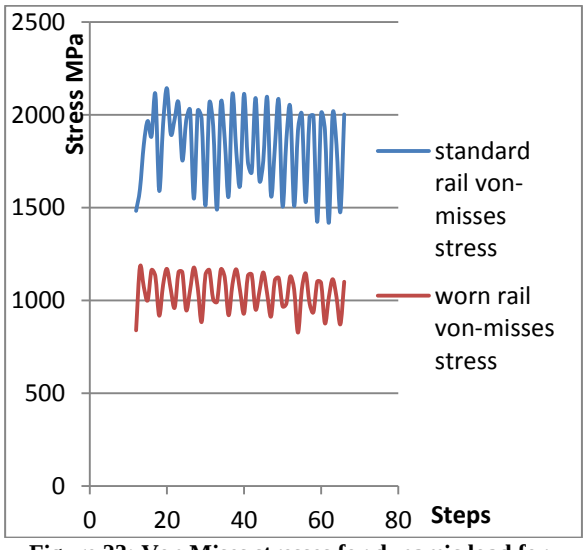

Figure 23: Von Mises stresses for dynamic load for standard and worn rail

Conicity which is the outcome of the mutual fit of the rail and wheel, is known as the “equivalent cone angle” of a specific track-wheelset combination. When a wheelset moves in one direction or the other, it may automatically guide itself back to a path halfway between the rails. High conicity can cause dynamic instability, sometimes known as "hunting," which significantly affects the ride and can harm the track. The worn rail case improves the fit between the wheel and rail, reducing contact stresses. Therefore, decreasing contact stresses will be followed by a rise in conicity which leads to a stress increase at the edges where the wheels make more contact and instability in the track moving. [19]

Credit Authorship Contribution Statement:

Ismail Mohsen: Methodology, Writing Original Draft, Software.
Ashraf El-Sabbagh: Conceptualization, Review and Editing, Supervision.
Ahmed Adel Turk: Supervision, Review, and Editing.

Declaration of Competing Interest

The writers claim to not know about competing financial interests or personal relationships that could have appeared to influence them.

4 CONCLUSIONS

In this research, the dynamic and static contact studies of a standard ENR UIC54, a real worn ENR UIC54 rail profile, and a wheel profile as per Egyptian standards were carried out through 3D FEA. Analysis was carried out using 100kN wheel loads based on the conditions in which the wheel is on the sleeper. contact stresses, pressure, and fatigue lifetime for static and dynamic conditions are figured comparatively. A 3D laser scanner is used to evaluate wear for the rail profile at the port-said railway station so a real worn rail profile is used in this study. Using stress distribution obtained through FEM analysis, the effects of the change in Egyptian rail profiles with ENR New locomotives’ wheel on the contact stress is investigated. Contact stresses for the worn rail profile are up to 40% lower than those for an unused ENR rail profile. These results happened as the worn rail has a larger contact area than the standard rail. Larger contact area gives less contact stress than smaller contact area. A wider contact area can also help distribute the wear more evenly across the surface of the rail and the wheel. This can lead to reduced wear and tear on both the rail and the wheel promoting longer service life. While worn rails might have less stress distribution due to the increased contact area at the rail head, the increased conicity can counteract this advantage by causing higher localized stresses at the edges where the wheels make more contact. New research on fracture development and spread in the rail as well as on abrasion in the rail and wheel will be performed after this study. It will investigate how conicity affects wheel deformation and wheel edge stresses.

5 REFERENCES

[1] "Hertz, H. R. 'On the contact of two elastic solids.' Macmillan & Co. Cap 5 (1882): 146-162.".

[2] "Fischer, Franz Dieter, and M. Wiest. 'Approximate analytical model for Hertzian elliptical wheel/rail or wheel/crossing contact problems.' Journal of tribology 130, no. 4 (2008).".

[3] "Tanaka, Naoyuki. 'A new calculation method of Hertz elliptical contact pressure.' J. Trib. 123, no. 4 (2001): 887-889.".

[4] "Antoine, Jean-Francois, Codrut Visa, Christophe Sauvey, and Gabriel Abba. 'Approximate analytical model for Hertzian elliptical contact problems.' Journal of Tribology 128, no. 3 (2006): 660-664.".

[5] "Telliskivi, Tanel, and Ulf Olofsson. 'Contact mechanics analysis of measured wheel-rail profiles using the finite element method.' Proceedings of the Institution of Mechanical Engineers, Part F: Journal of Rail and Rapid Transit 215, no. 2 (2001): 65-72.".

[6] "Sladkowski, Aleksander, and Marek Sitarz. 'Analysis of wheel–rail interaction using FE software.' Wear 258, no. 7-8 (2005): 1217-1223.".

[7] "Soemantri, Satryo, Wiratmaja Puja, Bagus Budiwantoro, Made Parwata, and Dirk J. Schipper. 'Solution to Hertzian contact problem between wheel and rail for small radius of curvature.' Journal of Solid Mechanics and Materials Engineering 4, no. 6 (2010): 66".

[8] "Butini, E., L. Marini, E. Meli, A. Rindi, M. C. Valigi, and S. Logozzo. 'Development and validation of wear models by using innovative three-dimensional laser scanners.' Advances in Mechanical Engineering 11, no. 8 (2019): 1687814019870402.".

[9] "Valigi, Maria Cristina, Silvia Logozzo, and Gabriele Canella. 'A new automated 2 DOFs 3D desktop optical scanner.' In Advances in Italian Mechanism Science: Proceedings of the First International Conference of IFToMM Italy, pp. 231-238. Springer Internati".

[10] "Valigi, M. C., S. Logozzo, E. Butini, E. Meli, L. Marini, and A. Rindi. 'Experimental evaluation of tramway track wear using 3D metrological optical scanners.' Tribology-Materials, Surfaces & Interfaces 15, no. 2 (2021): 150-158.".

[11] "Yan, W., and F. D. Fischer. 'Applicability of the Hertz contact theory to rail-wheel contact problems.' Archive of applied mechanics 70 (2000): 255-268.".

[12] "H.L. Whittemore, and S.N. Petrenko, Technical Paper 201. National Bureau of Standards, 1921".

[13] "SHARMA, SUDHANSHU. 'ANALYSIS OF CONTACT STRESSES FOR RAILWHEEL INTERFACE.' PhD diss., 2019.".

[14] "Özdemir, Yalcin, and Petr Voltr. 'Analysis of the wheel and rail frictionless normal contact considering material parameters.' Journal of Applied Mathematics and Computational Mechanics, volume 15, issue: 2 (2016).".

[15] "Suresh, Subra. Fatigue of materials. Cambridge university press, 1998.".

[16] "Jiang, Yanyao, and Huseyin Sehitoglu. 'A model for rolling contact failure.' Wear 224, no. 1 (1999): 38-49.".

[17] "Srivastava, J. P., P. K. Sarkar, and V. Ranjan. 'Contact stress analysis in wheel–rail by Hertzian method and finite element method.' Journal of The Institution of Engineers (India): Series C 95 (2014): 319-325.".

[18] "Jagadeep, B., P. Kiran Kumar, and K. Venkata Subbaiah. 'Stress analysis on rail wheel contact.' International Journal of Research in Engineering, Science and Management 1, no. 5 (2018): 47-52.".

[19] "Smallwood, R., J. C. Sinclair, and K. J. Sawley. 'An optimization technique to minimize rail contact stresses.' Wear 144, no. 1-2 (1991): 373-384.".